Rezumat

T10: Transportul si controlul impuritatilor grele (W) in centrul plasmei si in SOL.
Principalul obiectiv, validarea importantei noului concept al drifturilor ascunse asupra trasportului ionilor de W, a fost indeplinit ca rezultat al unui studiu detaliat al interactiei neliniare a acceleratiei paralele cu transportul perpendicular. Efectul principal consta din generarea unei curgeri radiale, ce este suficient de puternica pentru a contribui la dinamica ionilor de W in plasmele existente si in ITER.

T11 Confinarea, transportul și controlul ionilor rapizi în condiții relevante pentru ITER.

A fost investigat efectul turbulenței de drift asupra transportului ionilor rapizi în plasmele tokamak de tip AUG sau ITER în prezența perturbațiilor rezonanțelor magnetice (RMP). S-a construit un model de transport și o metodă de generare a câmpurilor aleatorii gaussiene pentru implementarea metodei simularilor numerice directe (DNS). Rezultatele numerice au relevat supresia transportului turbulent pentru ionii rapizi și un cuplaj sinergetic care duce la creșterea difuziei de tip RMP. Ne-omogenitatea câmpului magnetic dă naștere la asimetrii ale efectele difuzive și, implicit, la apariția unui drift radial.

Summary

T10: Transport and control of W and heavy impurities in the core and SOL.
The main objective, the assessing the importance of the new concept of hidden drifts on W transport, was accomplished as result of a detailed study of the nonlinear interaction of the parallel acceleration with the perpendicular transport. The main effect consists of the generation of a radial pinch, which is rather strong to contribute to the W ion dynamics in the existing plasmas and in ITER conditions.

T11: Fast ion confinement, transport and control under ITER relevant conditions.
The effect of drift turbulence in the presence of RMP on fast ion transport in AUG or ITER-like tokamak plasmas has been investigated. We have developed a transport model as well as a new method to generate Gaussian random fields for the use of direct simulation method (DNS). Numerical results have revealed a suppresion of turbulent transport for fast ions and a sinergistic mechanism leading to an increase of RMP-type diffusion. Magnetic field inhomogeneities lead to a small radial drift.

Detailed results

T10: Transport and control of W and heavy impurities in the core and SOL.

A detailed analysis of the turbulent transport of heavy impurities in the conditions of the AUG plasmas was performed in the frame of a test particle model. A particular attention is devoted to the nonlinear interaction of the parallel accelerated motion of the W ions with the perpendicular transport.

We have analysed the effects of the parallel acceleration a_z on the diffusion coefficients and on the radial pinch velocity. The acceleration scales as $a_z \sim Z/A$, where Z is the ionization rate and A is the mass number of the ions. Thus, it is smaller for the W impurities than for plasma ions. The factor Z/A varies in the interval $(0.05,\ 0.33)$ for the W impurities, while it has the value 0.5 for the deuterium. Surprisingly, we have found that the effect of a_z can be significant for W impurities, while it is negligible for deuterium ions.

The main effect of the nonlinear interaction of the parallel accelerated motion with the perpendicular transport consists of the generation of a radial pinch velocity V_x . This is a new, rather unexpected phenomenon. The parallel acceleration is expected to influence impurity transport through the modification of the parallel decorrelation time. We have shown that, beside this direct effect, a much stronger coupling of the parallel accelerated motion to the radial transport appears. It consists of the perturbation of hidden drifts (HDs). The HDs are a pair of opposite velocities in the radial direction that appears in the presence of a poloidal average velocity [1]-[2]. This quasi-coherent motion has zero average and does not determine a convective velocity in the case of the ExB drift. The stochastic parallel acceleration perturbs the equilibrium of the HDs leading to a radial pinch.

The transport Model

Most of the analysis is performed in the frame of a test particle stochastic model, which is shown to be the minimal model that yields the pinch V_x . We study impurity transport in the slab approximation, at the low field side of the plasma. The dimensionless equations for the impurity ion trajectories are

$$\frac{dx}{dt} = -K_* \, \partial_y \varphi(\mathrm{x}, z, t), \; \frac{dy}{dt} = K_* \, \partial_x \varphi(\mathrm{x}, z, t) + V_p, \tag{1}$$

$$\frac{dz}{dt} = \frac{1}{\sqrt{A}} v_z, \;\; \frac{dv_z}{dt} = -P_a \, \partial_z \varphi, \tag{2}$$

where the first term in Eqs. (1) is the stochastic drift determined by the electric field of the turbulence $-\nabla\phi(\boldsymbol{x}(t), z(t), t)$ and the second term V_p is a poloidal average velocity that can be produced by the magnetic drifts or plasma rotation. The parallel motion includes the variation of the velocity determined by the stochastic acceleration a_z. Dimensionless quantities are used, with the units: $\rho_i = v_{thi}/\Omega_i$, the Larmor radius of the protons (for the perpendicular distances, for the correlation lengths λ_x, λ_y and for $1/k_0$), a, the small radius of the plasma (for the parallel distances and for the correlation length λ_z), $\tau_0 = a/v_{thi}$ (for time and for τ_d), A_φ, the amplitude of the potential (for the potential φ), $V_* = \rho_i v_{thi}/a$ (for the perpendicular velocities and V_d) and $v_{thW} = v_{thi}/\sqrt{A}$ (for the parallel velocity of the W ions). $v_{thi} = \sqrt{T_i/m_p}$ is the thermal velocity of protons with temperature T_i and mass m_p and $\Omega_i = eB/m_p$ is the cyclotron frequency of the protons. The correlation lengths , λ_x, λ_y, λ_z and time τ_d appear in the Eulerian correlation of the (Gaussian) stochastic potential $\varphi(x, z, t)$

$$E(x, z, t) \equiv \langle \varphi(0,0,0) \;\, \varphi(x, z, t) \rangle. \tag{3}$$

It is modelled by

$$E(x, z, t) = \partial_y \left[exp\left(-\frac{x^2}{2\lambda_x^2} - \frac{y^2}{2\lambda_y^2} - \frac{z^2}{2\lambda_z^2} \right) \frac{sin(k_0 y)}{k_0} \right] exp\left(-\frac{t^2}{4\tau_d^2} \right), \tag{4}$$

which corresponds to the drift type turbulence.

The main characteristics of the model appear in the dimensionless parameters evidenced in the dimensionless equation :

$$K_* = \Phi \frac{a}{\rho_i}, \;\;\; \Phi = \frac{eA_\varphi}{T_i}. \tag{5}$$

$$V_p \equiv \frac{V_d}{V_*} = \frac{V_d}{v_{thi}} \frac{a}{\rho_i}, \qquad P_a \equiv \Phi \frac{Z}{\sqrt{A}}, \tag{6}$$

where K_* is the dimensionless measure of turbulence amplitude, V_p is the poloidal velocity and P_a is the measure of the acceleration a_z.

The energy of the ions normalized with the temperature T_i is $W = \frac{v_z^2}{2} + Z\Phi\phi$. It is the invariant of the motion in three-dimensional static potentials $\phi(x, z, t)$. This constraint influences the transport for $\tau_d \to \infty$, and its effects persist in the case of potentials with slow time variation (large τ_d). We note that the energy is dominated by the potential energy for the W ions with large Z, even at small turbulence amplitudes ($\Phi \sim 10^{-2}$).

Theoretical methods

We use two theoretical methods for determining the pinch velocity and the transport coefficients, the direct numerical simulations (DNS) and the decorrelation trajectory method (DTM) [3].

A three-dimensional DNS code for ion trajectories and for the calculation of the statistical Lagragian quantities was developed. It is based on an original method for generation of Gaussian random fields that essentially increase the stochasticity compared to the well known fast Fourier representation, by including random wave numbers instead of fixed values on a grid. We have shown [*] that the representation (FRD) provides fast convergence of the Eulerian statistics of the generated fields, as well as of the Lagrangian statistics of trajectories. In particular, it was proven that a convergence level with a few percents error can be achieved with a number of waves $N_c \sim 10^d$ and a number of realizations (trajectories) $M \sim 10^4$, where $d = 4$ for time dependent potentials and $d = 3$ for $\tau_d \to \infty$. Also, it is worth mentioning that such representations are able to reproduce with high accuracy the conservation laws of motion as well as certain Lagrangian statistical invariants.

The properties of the representation (FRD) enables to use commonly in the present simulations $N_c \sim 1 - 5 \times 10^3$ waves. The dimension of the statistical ensemble is usually set to $M \sim 10^5$ realizations (trajectories) which gives small statistical fluctuations. The numerical integration scheme used is a forth order Runge-Kutta method which preserves well the energy with a minimal numerical effort. Typical number of steps is 600 for the integration time $t = 30$. Depending on the integration time and on the type of turbulence (frozen, or not), the usual CPU times on personal computer are $t_{CPU} \sim 2 - 20$ hours per run. Detailed analyses of the statistical and numerical precision of the DNS code and of the dependence of the errors on N_c , M are presented in the Paper [*].

The DTM [3] is a semi-analytical approach that provides approximate evaluations of the transport characteristics. It is able to describe both the random and the quasi-coherent components of the trajectories [4]. The latter are determined by the finite correlation lengths of the stochastic potential and depend on the structure of the correlated zone that is described by the shape of the EC. The basic DTM is developed here by introducing the parallel acceleration. It is described in the Paper [**]

The DTM is used for identifying and understanding qualitatively the effects of the parallel acceleration and the new pinch mechanism, while the quantitative properties of the radial velocity V_x and of the diffusion coefficient D_x are determined using the much more accurate results provided by DNS.

Effects of the parallel acceleration

The effects of the parallel acceleration on the heavy impurity transport are identified by comparing typical results of the transport model with those obtained for deuterium ions and for W ions in two-dimensional potentials. The variation of the parallel velocity determines by the acceleration modifies the parallel decorrelation time (especially at large Z). It becomes a function that depends on all the parameters of the parallel motion. It can be approximated by

$$\tau_z^\infty(W, Z, \Phi, \lambda_z) \cong \lambda_z \sqrt{A}/v_z^{eff}, \tag{7}$$

which is a decreasing function of W, Z, Φ and an increasing function of λ_z (as λ_z^α with $\alpha > 1$).

The influence of the decorrelation time on the diffusion is different in the quasilinear ($\tau_z^\infty < \tau_{fl}$) and the trapping ($\tau_z^\infty > \tau_{fl}$) regimes. The asymptotic diffusion coefficient scales as

$$D_x^\infty \sim \begin{cases} \Phi^2 \tau_z^\infty, & \tau_z^\infty < \tau_{fl} \\ \Phi^\gamma \tau_z^{\gamma-1}, & \tau_z^\infty > \tau_{fl} \end{cases}, \tag{8}$$

where $0 < \gamma < 1$.

The effects of the interaction of the parallel motion with the perpendicular transport through the parallel decorrelation explain the results obtained for the diffusion coefficients. The influence of the parallel acceleration is negligible for the D ions and noticeable for W ions. The strongest difference appears due to the dependence of τ_z^∞ on the mass number, which leads to values of τ_z^∞ that are larger by a factor 10 for the W ions compared to the D ions. The diffusion is usually in the trapping regime for the W ions to much smaller D_x^∞ for the W ions compared to D ions.

The pinch mechanism

The physical processes that determine the generation of the radial pinch are examined using the DTM. We have shown [1], [2] that a special quasi-coherent effect, that is neither structure nor flow, appears in the stochastic transport in the presence of an average poloidal velocity V_p . It consists of two average radial velocities in opposite directions, which exactly compensate. This pair of drifts are named in [1] hidden drifts (HDs) because they do not yield an average velocity in these conditions.

The HDs are essentially determined by the existence of average displacements of the trajectories that start from same values of the potential φ^0 , and by the special property of these conditional averages $\langle x(t)\rangle_{\varphi^0}$ of having the sign correlated to the sign of φ^0. The conditional displacements $\langle x(t)\rangle_{\varphi^0}$ are zero in the case of the motion determined only by the electric drift ($V_p = 0$) , but they have finite values in the presence of an average poloidal velocity V_p . In the absence of the parallel acceleration (two-dimensional potentials), $\langle \mathrm{x}(t)\rangle_{\varphi^0}$ is an anti-symmetrical function of φ^0 and it leads, by integration over φ^0, to zero average displacement. This special type of quasi-coherent motion is generated by the average poloidal velocity V_p, which determines strong modifications of the contour lines of the total potential $\varphi_t(\mathrm{x}) = \varphi(\mathrm{x}) + xV_p$.

The average displacements conditioned by the sign of the initial potential

$$\langle x(t)\rangle_+ = \int_0^\infty d\varphi^0 \langle x(t)\rangle_{\varphi^0}, \quad \langle x(t)\rangle_- = \int_{-\infty}^0 d\varphi^0 \langle x(t)\rangle_{\varphi^0} \tag{9}$$

determine two opposite radial velocities V_+, V_- that exactly compensate $V_+ + V_- = 0$ due to the anti-symmetry of $\langle x(t)\rangle_{\varphi^0}$ with respect to the initial potential φ^0 (see [1], [2] for details). The heavy ions with large ionization rates Z have smaller acceleration, but also a much higher potential energy (larger than for D ions by the factor Z). Then, even for small amplitudes of the turbulence (Φ of the order 10^{-2}), the trajectories cannot reach the maxima of the stochastic potential, because the invariance of the energy (W) imposes $W - Z\Phi\varphi^0 = v_z^2/2 > 0$. The result is the cut of $\langle x(t)\rangle_{\varphi^0}$ at large φ^0. A strong symmetry breaking of the conditional displacements is produced at large Z, which determines non-symmetrical conditional displacements (9) and an average radial motion $\langle x(t)\rangle$. The latter yields an average radial velocity $V_x(t)$. The maximum allowed potential φ_{max} decreases with the increase of Z, which leads to the increase of the average displacement and of the pinch velocity V_x^{∞} . *This explains the significant pinch velocity produced by the parallel acceleration for W ions.*

Ion collisions and the gradient of the confining magnetic field are not essential ingredients in this mechanism and are not included in the minimal model analyzed here. However, they could interfere with the HDs by changing their amplitude and symmetry.
We have evaluated the effects of collisions using the DTM. The mechanism of the pinch velocity relies on the HDs, a quasi-coherent component of the motion. Collisions usually contribute to the enhancement of the random characteristics at the expense of the coherent ones. Moreover, in the case of heavy ions with large Z, the collision frequency ν and diffusion coefficient $d_c^{\perp}$ are much larger than for plasma ions

$$d_c^{\perp} = \sqrt{A}\frac{a}{\lambda_{mfp}}, \quad \nu = \frac{Z^2}{\sqrt{A}}\frac{a}{\lambda_{mfp}} \tag{10}$$

The effect of collisions on the pinch mechanism is exemplified in Fig. 1, where the average radial displacement is presented together with its conditional components in Eq. (9) for several values of the perpendicular collisional diffusion coefficient. One can see that $|\langle x(t)\rangle|$ decreases with the increase of $d_c^{\perp}$, which determines the decrease of the pinch velocity V_x^{∞}. The collision effect depends on the sign of the initial potential ($\langle x(t)\rangle_+$ and $\langle x(t)\rangle_-$ have different dependences on $d_c^{\perp}$). Thus, ion collisions have significant attenuation effect on the coherent motion that produce the HDs, but the pinch mechanism survives even at large collisional diffusion. This estimation finds an attenuation factor of the order 2 for a rather large interval of $d_c^{\perp}$.

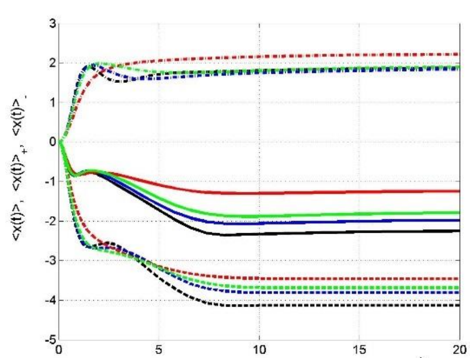

Fig. 1. *Effect of collisions. The average radial displacement $\langle x(t)\rangle$ (solid lines) with its conditional in Eq. (9)*

(dashed-dotted and dashed lines) as functions of time for $d_c^{\perp}$=0 (black), 0.3 (blue), 4.7 (green) and 11.8 (red).

Another process that could hinder the acceleration induced pinch is produced by the gradient of the magnetic field B, $dB/dx \cong B/R$, where R is the major radius of the plasma. It generates a radial pinch [5] that could influence the symmetry breaking of the HDs. We have found that the effect appears, but it is negligible for large size plasmas with $a/\rho_i ? 100$.

Scaling laws of the radial pinch and diffusion coefficient

The properties of the pinch velocity V_x and its dependence on the main parameters of the model are determined using the more accurate results of the DNS. The study is focused on the scaling of V_x with the main parameters of the model. The results are analyzed and physical explanations are derived.

We take under scrutiny a generic case of W ions in a ITER like plasma such that the mass of the ion is $A = 184$ and $\rho/a = 1/500$. The effective impurity charge is $Z = 40$, its energy $W = 1$ and the turbulence amplitude $\Phi = 0.03$ which implies $K_s = 15$ and $P_a = 0.09$. The others parameters of the model : $\lambda_x = 2, \lambda_y = 2, \lambda_z = 0.5, V_p = 1, \tau_d = 5$. These values are considered a basic configuration around which the parameters are individually varied during numerical simulations. We do that, in order to understand how the diffusion and the radial pinch depend on physical inputs.

The asymptotic radial velocity V_x^{∞} is shown in Fig. 2 (left panel) as function of Φ. The pinch is negative (inward) for the whole range of Φ and it increases with Φ. The dependence is approximately linear for $\Phi \le 0.04$, and a tendency of saturation can be observed at larger Φ. The asymptotic diffusion coefficient D_x^{∞}increases with the increase of Φ according to the law $D_x^{\infty} \sim \Phi^{\gamma}$ with $\gamma = 1.5$, as seen in Fig. 2 (right panel). The values $1 < \gamma < 2$ define the super-Bohm regime. Such regime is unusual in the presence of trajectory trapping or eddying, which yields the scaling (8) with $0 < \gamma < 1$. This stronger increase of D_x^{∞} is the effect of the parallel acceleration through the effective decorrelation time τ_z^{∞} . The latter is a decreasing function of Φ. Thus, the super-Bohm regime is the result of trajectory trapping coupled to the parallel accelerated motion.

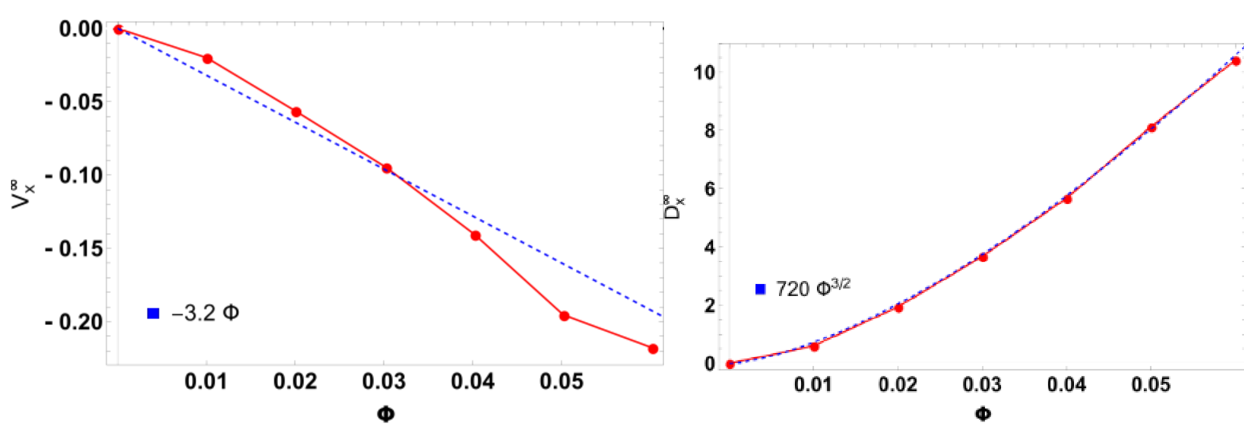

Fig. 2. *W transport dependence on turbulence amplitude : the asymptotic pinch velocity (left panel) and the diffusion coefficient (right panel).*

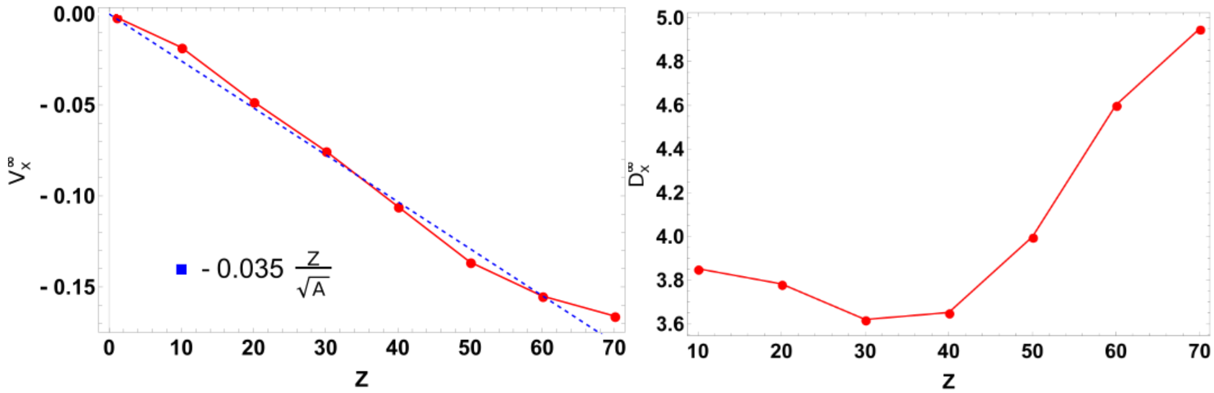

Fig. 3: *W transport dependence on the ionization rate Z : the asymptotic pinch velocity (left panel) and the diffusion coefficient (right panel).*

The mechanism of generation of the radial pinch depends essentially on the product $Z\Phi$. Thus, the ionization rate has a similar effect with the amplitude Φ of the turbulence. As seen in Fig. 3 (left panel), the pinch velocity has an approximately linear increase followed by the tendency of saturation, a behavior that is similar to the dependence on Φ (Fig. 2 (left panel)). The diffusion coefficient shown in Fig 3 (right panel) has a more complicated dependence on Z, but the variation of D_x^∞ on the relevant range of Z is small (of the order $\pm 20\%$ of the average). The influence of Z on the diffusion is produced through the effective parallel decorrelation time τ_z^∞ that depends on Z.

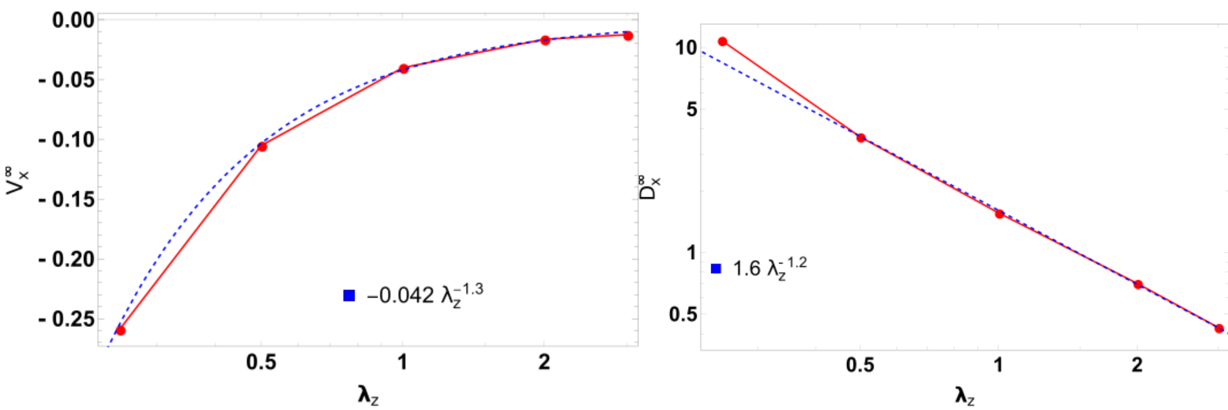

Fig 4: *W transport dependence on the parallel correlation length λ_z : the asymptotic pinch velocity (left panel) and the diffusion coefficient (right panel).*

The pinch mechanism analyzed here appears only in three-dimensional stochastic potentials. But, as discussed, V_x^∞ essentially results from the symmetry breaking of the HDs determined by the energy conservation. The potential energy does not dependent on λ_z, which means that a finite λ_z is necessary, but its direct quantitative influence on the pinch mechanism is small. However, λ_z has a strong influence on the transport through the parallel decorrelation time τ_z^∞ that increases with λ_z faster than linearly. It explains the large decrease rate of both V_x^∞ and D_x^∞ seen in Fig. 4, which shows that $V_x^\infty \sim \lambda_z^{-1.3}$ and $D_x^\infty \sim \lambda_z^{-1.2}$. Thus, λ_z determines the decrease of V_x^∞ and D_x^∞ only through the modification of the τ_z^∞.

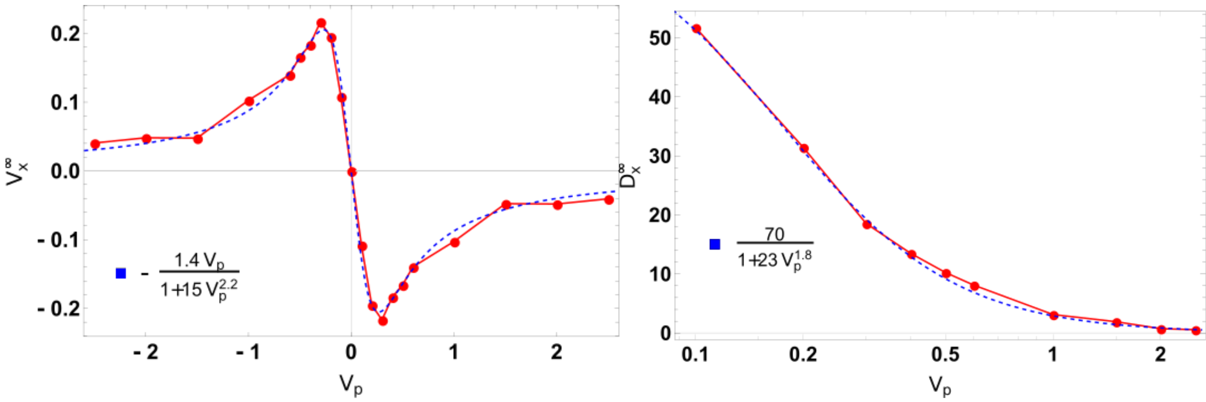

Fig. 5: *W transport dependence on the poloidal velocity V_p : the asymptotic pinch velocity (left panel) and the diffusion coefficient (right panel).*

The poloidal average velocity is the source of the hidden drifts. It has a strong influence on both the pinch velocity and the diffusion coefficient, as seen in Fig. 5. The equations of motion are invariant at the change $V_p \to -V_p$ and $x \to -x$, which implies that the conditional displacements and the HDs change their sign when $V_p \to -V_p$. Thus, the pinch velocity V_x^∞ is an anti-symmetrical function of V_p, as seen in Fig. 5 (left panel). V_x^∞ is linear in V_p at small V_p, it has a maximum at $V_p \sim 0.3$ and a long tail with $V_x^\infty \sim V^{-1.2}$ at large V_p. The direction of the pinch produced by the parallel acceleration can be changed from inward to outward by inversing the orientation of the poloidal velocity. The diffusion coefficient is strongly influenced by V_p, which determines a large decrease of D_x^∞ , as seen in Fig. 5 (right panel). Thus, V_p has a special effect on the transport, different compared to the other parameters. The pinch velocity V_x^∞ is modified because V_p influences the amplitude of the HDs. The diffusion coefficient D_x^∞ is modified because V_p influences the structure of the contour lines of the total potential.

Evaluation of the relevance of the acceleration induced pinch for JET, AUG and ITER

The physical domains of the main parameters of the transport model were explored for evaluating the scaling laws and for obtaining the range of the normalized pinch velocity and diffusion coefficient. The typical values of $|V_x^\infty|$ are in the interval $(0.05,\ 0.25)$.

The relevance of the acceleration induced pinch velocity appears more clearly in physical units. The typical normalized values determine different velocities for present plasmas (ASDEX Upgrade, JET) and ITER conditions. The main difference (concerning V_x^∞) is the electron temperature. Due to the time-scale separation of the atomic and transport processes, the W impurities are in coronal equilibrium. The fractional abundance of each ionization stage is a function of the electron temperature that is practically not influenced by the transport [6]. This determines different ranges of the ionization rates for the present plasmas and ITER. In the first case Z varies from boundary to the center in the interval $(20,\ 48)$, while in the second case the interval is $(45,\ 63)$. Typical values of Z in the core plasma are $Z = [43,\ 44,\ 57]$, where the first value in this and the following triads corresponds to ASDEX Upgrade, the second to JET and the third to ITER. This determines normalized values of the pinch velocity of the order $|V_x^\infty| \approx [0.10,\ 0.11,\ 0.15]$. Using typical parameters of these plasmas, the pinch velocities are of the order $|V_x^\infty| \approx [160,\ 110,\ 194]\ m/sec$. Thus, the pinch velocity is larger in the ITER plasmas roughly by 50% at similar parameters of the turbulence and poloidal velocity. The convection time to plasma center is very small $\Delta t_c = a/V_x^\infty \approx [4,\ 11,\ 10]\ msec$. Convection dominates diffusion in all cases, because $\Delta t_c \ll \Delta t_{dif}$, where $\Delta t_{dif} = a^2/(2D_x^\infty)$ is the diffusive time. The ratio $r = \Delta t_c/\Delta t_{dif}$ is $r \approx [0.18,\ 0.10,\ 0.07]$.

These values of the pinch velocity are evaluated in the frame of the minimal model (1)-(2). They only show that the effect produced by the parallel acceleration is very large in these ideal conditions. Collisions determine the attenuation of V_x^∞ by a factor of the order 2. Also, interactions with other pinch mechanisms and neoclassical aspects can strongly modify these values. Compared to the results obtained from complex models and simulations, this pinch velocity is larger by an order of magnitude (see, for example, the very recent paper [7], where the central accumulation of the W ions seen in Fig. 3 appears in hundreds of $msec$, corresponding to pinch velocities of the order of $10m/sec$).

We underline that the dependence of V_x^∞ on V_p (Fig. Figure 5 (left panel)) could provide a very efficient control possibility. The change of V_p from the direction of the electron to the ion diamagnetic velocity determines the inversion of the pinch from inward to outward direction. A strong variation of V_x^∞ with V_p exists at small $|V_p| < 0.5$, which shows a high sensitivity of the pinch velocity to the poloidal velocity.

References

[1] Vlad M. and Spineanu F. 2018 Hidden drifts in turbulence *Europhysics Letters (EPL)* 124, 60002

[2] Vlad M. and Spineanu F. 2018 Combined effects of hidden and polarization drifts on impurity transport in tokamak plasmas *Phys. Plasmas* 25 092304

[3] Vlad M., Spineanu F., Misguich J. H. and Balescu R. 1998 Diffusion with intrinsic trapping in 2-d incompressible velocity fields *Phys. Rev. E* 58 7359

[4] Vlad M. and Spineanu F. 2017 Randon and quasi-coherent aspects in particle motion and their effects on transport and turbulence evolution New Journal of Physics 19 025014

[5] Vlad M., Spineanu F. and Benkadda S. 2006 Impurity pinch from a ratchet process Phys. Rev. Lett. 96 085001

[6] Putterich T., Neu R., Dux R., Whiteford A. D. and O'Mullane M. G. 2008 Modelling of measured tungsten spectra from ASDEX Upgrade and predictions for ITER Plasma Phys. Control. Fusion 50 085016

[7] Casson F.J. et al (JET EFDA Contributors and ASDEX-Upgrade Team) 2020 Predictive multi-channel flux-driven modelling to optimise ICRH tungsten control and fusion performance in JET Nucl. Fusion 60 066029

T11: Fast ion confinement, transport and control under ITER relevant conditions

In present day tokamak devices, but especially in future D-T plasma experiments like ITER, there will be a significant population of supra-thermal fast ions with energies in the MeV range originating from the fusion reaction or from external heating mechanisms. As they are a crucial source of heat, momentum and current, it is important to understand and control the transport of such particles. Two particular mechanisms of transport are important in fusion plasmas: electrostatic turbulence and magnetic perturbations.

In the present work we intend to analyze the physical mechanisms behind this type of transport of fast ions using a test-particle transport model. The electrostatic turbulence and the RMPs are considered stochastic fields with known Eulerian statistics. Their characteristics serve as input parameters. The statistical nature of the model is tackled with a direct numerical simulation (DNS) method. The diffusion coefficients are computed as a quantitative measure of transport. Approximate scaling laws for diffusion are being explored.

Direct numerical simulations

The purpose of direct numerical simulations (DNS) is to investigate the turbulent transport as it is, without resorting to any approximations, closures, or supplementary models [1,2,3]. In our case, the Eulerian characteristics of turbulence are fully prescribed via the Gaussian statistics and the correlation function. Therefore, the goal of a DNS is to compute the characteristic trajectories of turbulence.

This is achieved constructing a statistical ensemble of Gaussian random fields (GRFs) with the correct correlation function. For each realization, the set of eqns. of the transport model is solved and a trajectory is obtained. The transport coefficients, diffusion and average velocity, are computed as simple statistical averages over the ensemble:

$$\langle v(t)\rangle = \frac{d\langle x(t)\rangle}{dt} \quad ; \quad D(t) = \frac{1}{2}\frac{d}{dt}\langle x^2(t)\rangle. \tag{1}$$

Gaussian random field generation

The DNS method, as described above, requires the generation of a large (infinite, in theory) ensemble of high dimensional potentials $\phi(x,y,z,t)$. This is not an easy numerical task and a DNS can be become very rapidly prohibitive in practice. For this reason we have searched actively for ways to improve the computational speed of GRF generation. We have focused on the theory of GRFs representations: we have developed a general theoretical setup [1] within which several numerical approximations of GRFs were constructed. All these methods approximate a GRF $\phi(x)$ as a superposition of elements:

$$\phi(x) = \sum_i \zeta_i\, F(x; a_i) \tag{2}$$

If the function F is a trigonometric function, the method is of Fourier type (F), if it is the square root of correlation is of Blob type (B). If the a_i are on an uniform grid, the method is fixed (F), if not, it is random (R). Finally, depending on the values of the ζ_i, the method can be discrete (D) or continuous (C). From all possible representations we have chosen for the present work the method called FRD [1]:

$$\phi(x) = L_k^{1/2} \sum_i \sqrt{S(k_i)}\, sin(k_i x + \frac{\pi}{4}\zeta_i) \tag{3}$$

where $S(k)$ is the spectrum of the random field, i.e. the Fourier transform of the correlation function $E(x)$. The wavenumbers k_i are randomly chosen within the compact support of the spectrum. The phases $\zeta_i = \pm 1$. The convergence of the FRD method is proven numerically [1]. In particular, we have shown that the convergence of Eulerian properties implies convergence of Lagrangian statistics. Small errors ($\sim 1\%$) can be achieved using a number of waves $N_c \sim 10\ d$ where d is the dimensionality of the space ($d = 4$ in our case). The dimension of the statistical ensemble is, usually, $N_p \sim 10^5$. Also, it is worth mentioning that such representations are able to reproduce with high accuracy the conservation laws of motion as well as certain Lagrangian statistical invariants. The numerical integration scheme used is a 4th order Runge-Kutta method which preserves well the energy with a minimal numerical effort. Depending on the integration time and on the type of turbulence (frozen, or not), the usual CPU times on personal computer are $t_{CPU} \sim 2 - 20\ h$ per run.

Transport Model

The motion of fast ions in a tokamak plasma can be described with a test-particle transport model [4] in a standard slab geometry setup $(\boldsymbol{x}, \boldsymbol{z}) = ((x, y), z)$, x, y, z representing the radial, poloidal and toroidal directions). Ion dynamics is driven by the turbulent stochastic potential $\phi(\boldsymbol{x}, z, t)$ and the RMP magnetic field $\boldsymbol{b}(\boldsymbol{x}, z, t)$. The poloidal and toroidal components of the magnetic perturbations are smaller than the radial one, thus, have little influence on the radial dynamics. Moreover, *Oz* is the only direction on which the characteristic length Λ_z of the RMP is comparable with the correlation length λ_z of the electric potential $\phi(\boldsymbol{x}, z, t)$. Thus, one can approximate the magnetic influence on transport with a stochastic RMP field $\boldsymbol{b}(\boldsymbol{x}, z, t) \approx b(z)\hat{e}_x$. The stochastic character of $b(z)$ is justified by the intrinsic noise of the RMPs and the random initial spreading of ions.

The system is immersed in a large toroidal, inhomogeneous, magnetic field $B\hat{e}_z$ which, at the turbulence scale, can be approximated as $B = B_0 \exp(-x/R)$. The RMP's amplitude is orders of magnitude smaller than the toroidal field $|b| \ll B_0$. Dealing with fast particles, collisions can be neglected. The gyro-averaging procedure $\langle * \rangle_g = T^{-1} \int_t^{t+T} * \, d\tau$ of Larmor rotation leads to the following equations of motion for the guiding-center $\left(\boldsymbol{X}_\perp(t), Z(t)\right) = \left\langle \left(\boldsymbol{x}_\perp(t), z(t)\right) \right\rangle_g$ of a fast ion:

$$\frac{dX_\perp}{dt} = \frac{\hat{e}_z \times \nabla_\perp \phi_g}{B} + \frac{v_z b_g}{B} \hat{e}_x + V_p \quad ; \qquad\qquad \frac{dZ}{dt} = v_z \tag{4}$$

The electrostatic turbulent potential $\phi(x, z, t)$ is modelled as a homogeneous Gaussian random field with known Eulerian correlation (EC) function $E(x, z, t) = \langle \phi(x, z, t)\phi(0,0,0) \rangle$ corresponding to drift type turbulence

$$E(\mathbf{x}, z, t) = A_\phi^2 \partial_y \left[\exp\left(-\frac{x^2}{2\lambda_x^2} - \frac{y^2}{2\lambda_y^2} - \frac{z^2}{2\lambda_z^2} \right) \frac{\sin(k_0 y)}{k_0} \right] T(t), \tag{5}$$

where A_ϕ is the amplitude of the potential fluctuations, $\lambda_x, \lambda_y, \lambda_z$ are the correlation lengths along the radial, poloidal and parallel directions, and k_0 is the dominant wave number. The function *T(t)* is the time correlation of the potential that is a decaying function of time with τ_d the decorrelation time

$$T(t) = \exp\left(-\frac{t^2}{4\tau_d^2}\right). \tag{6}$$

Similarly, for the RMP, the field is described as a Gaussian random field with known correlation function:

$$B(z) = A_\beta^2 \exp(-\frac{z^2}{2\Lambda_z^2}) \tag{7}$$

The gyroaveraging procedure has a negligible effect on the RMP field due to its large correlation length characteristic. Yet, it affects the electrostatic potential. Assuming that the fast ions are Maxwellian distributed one can show [5] that the gyro-averaged potential ϕ_g is described by an effective correlation function:

$$E^{eff}(x_\perp, t; v_z, \rho_f) = \int dk\, S_\phi(k_\perp, v_z t, t) e^{-k_\perp^2 \rho_f^2} I_0(k_\perp^2 \rho_f^2) e^{ik_\perp x_\perp} \tag{8}$$

where $\rho_f = v_f/\Omega_c$ is the thermal Larmor radius associated with the thermal velocity of fast ions v_f . The function $S(k_\perp, z, t)$ is the turbulence spectrum, the Fourier transform of the correlation function $E(x_\perp, z, t)$. The parallel velocity v_z remains a free parameter.

The folowing scalling is adopted in practice to scale the equations from the transport models : $(R, x, y, \lambda_x, \lambda_y, k_0^{-1}) \to \rho_i$, $(z, \lambda_z, \Lambda_z) \to L_{T_i}$, $\phi \to A_\phi$, $b \to \beta$, $\tau \to \tau_0$, $\rho_f \to \rho_i$ and $v_z \to v_{T_f}$. R is the major radius, Λ_z the RMP's correlation length, b the RMP field, v_z the parallel velocity, W the energy of the ion and v_{T_f} its associated thermal temperature. The latter is scaled with the bulk temperature T_i which defines also the thermal velocity $v_{T_i} = \sqrt{T_i/m_i}$ and the Larmor radius $\rho_i = v_{T_i}/\Omega_c$. Ω_c is the Larmor frequency $\Omega_c = |e|\, B_0/m$ and $L_{T_i}$the characteristic length of the ion temperature $L_{T_i} = |\nabla \ln v_{T_i}|^{-1}$. The resulting set of equations for the transport model is given in eqns. (9). We underline that this model is statistical by nature: the parallel velocities are Gaussian distributed with unit variance while the fields $\phi_g(x_\perp, z, t)$ and $b(z)$ are stochastic GRFs with prescribed spectra.

$$\begin{cases} \dfrac{dX(t)}{dt} = e^{\frac{X(t)}{R}} \left(-K_s \partial_y \phi_g + P_b v_z b(P_z v_z t)\right) \\ \dfrac{dY(t)}{dt} = K_s\, e^{\frac{X(t)}{R}}\, \partial_x \phi_g + V_p \\ S_\phi^{eff}(\mathbf{k}_\perp, \omega; v_z) = \dfrac{\tau_{eff}}{\sqrt{\pi}} e^{-\tau_{eff}^2 \omega^2} \dfrac{\lambda_x \lambda_y^3}{2\pi} k_y^2 e^{-\frac{k_x^2 \lambda_x^2}{2} - \frac{k_y^2 \lambda_y^2}{2}} e^{-\rho_f^2 \mathbf{k}_\perp^2} I_0(\rho_f^2 \mathbf{k}_\perp^2) \\ S_b(k_z) = \dfrac{\Lambda_z}{\sqrt{2\pi}} e^{-\frac{k_z^2 \Lambda_z^2}{2}} \\ K_s = \dfrac{q A_\phi}{T_i} \dfrac{L_{Ti}}{\rho_i}; \quad P_b = \dfrac{\beta}{B_0} \dfrac{L_{Ti}}{\rho_i} \dfrac{v_{Tf}}{v_{Ti}}; \quad V_p = \dfrac{V_p L_{Ti}}{v_{Ti} \rho_i} \\ P_z = \dfrac{v_{Tf}}{v_{Ti}}; \quad \tau_{eff}^{-2} = \tau_c^{-2} + 2 P_z^2 v_z^2 / \lambda_z^2 \end{cases} \tag{9}$$

Physical picture and analytical results

We take under analytical and numerical analysis 4 particular characteristics of the transport model in order to investigate their impact on transport coefficients. The conclusions of our analysis are:

- the inhomogeneous B field leaves the diffusion unchanged while inducing a small radial pinch

$$\frac{d\langle x(t)\rangle}{dt} = \frac{D_x(t)}{R} \tag{10}$$

These pinch values are small so they do not dominate the transport. Yet, they reflect a natural tendency of an effective ion drift towards the walls due to magnetic field variations.

- the RMP field *b(z)* contributes to the radial transport as a velocity field $V_b(t;v_z) = P_b v_z b(P_z v_z t)$. The results is a naural RMP diffusion which can be analytically estimated :

$$D_b(t) = \frac{1}{2}\frac{d}{dt}\langle x_0^2(t)\rangle = \int dv_z\ P(v_z)\int_0^t d\tau \langle V_b(\tau;v_z)V_b(t;v_z)\rangle = \frac{P_b^2 t}{\sqrt{1+P_z^2\frac{t^2}{\Lambda_z^2}}} \xrightarrow{t\to\infty} \frac{P_b^2}{P_z}\Lambda_z \tag{11}$$

- the effect of finite Larmor radius on the turbulent transport has been considered before in some simplified cases [5]. The main outcome, confirmed by gyrokinetic simulations, is that the diffusion decays with the energy of the particles. The effect is small for ”slow” ions $T_f \sim T_i$ and increases with their energy leading to a generic dependency $D \sim W^{-1/2}$ at large energies. A good fit for the effect of finite Larmor radius on diffusion is interpolated by the following function

$$\frac{D_x^\infty(\rho)}{D_x^\infty(0)} = \left(\frac{2\rho^2/\lambda_c^2+1}{(4\rho^2/\lambda_c^2+1)^{3/2}}\right)^\gamma$$

(12)

- the coupling between turbulence and RMP is non-linear and leads to a synergistic mechanisms of diffusion which can be quantified through a term $D_{\phi b}$ which can be roughly estimated as :

$$D_{\phi b} \sim \frac{\Lambda_z P_b^2}{P_z}\frac{K_s^2 V_{eff}^2}{\lambda_{\{eff\}}^2} f(\rho_f)$$

(13)

The effects of the synergistic mechanisms can be seen ”at work” in Fig. 1 where was plotted, from a realistic simulation of the transport model (4), the total diffusion *D(t)* (red), the pure *E×B* diffusion $D_\varphi(t)$ (in blue, decaying asymptotically to 0) the pure RMP induced diffusion $D_b(t)$ (in black, dashed line) and the difference, the non-linear coupling term $D_{\varphi b}(t)$ (green). The case with $\tau_c \to \infty$ was chosen to ensure that the $D_{\phi b}^0 \to 0$. One can observe how $D_{\varphi b}$ is non-zero and almost everywhere positive, which supports the idea of synergistic coupling. The total diffusion serves as a measure of the confinement degradation. The quantity $D_{\varphi b}$ quantifies the effect of RMP on turbulent transport.

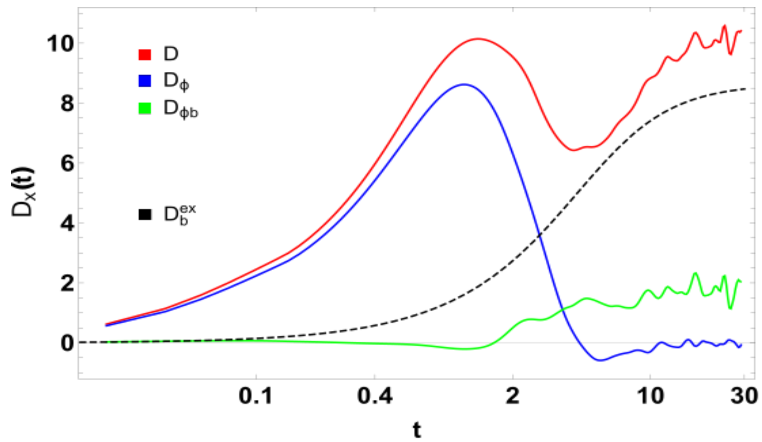

FIG. 1: Running diffusion profiles for each component D (red), D_b (black, dashed), D_ϕ (blue) and the coupling term $D_{\phi b}$ (green), obtained in a DNS simulation

Numerical results

A series of DNSs are performed using the transport model (13) in full basic scenario: $\lambda_x = 4$, $\lambda_y = 2$, $\tau_c = 10$, R/a = 3, L_{Ti} = R/5, V_p = 1, W = 10, K_s = 9, $\beta/B_0 = 10^{-3}$ which implies $P_b \approx 0.47$, $P_z \approx 1.58$. These values are relevant for ITER. A few physically relevant quantities for the fast ions or for the stochastic driving fields are varied around the basic scenario: the turbulence amplitude $\Phi = eA_\phi/T$, the poloidal velocity V_p, the RMP amplitude β, the correlation time τ_c and the thermal energy of fast ions W.

- Turbulence : The effect of turbulence amplitude $\Phi = qA_\phi/T_i$ on diffusion coefficients is shown in Fig. 6a against the RMP contribution D_b^∞ (in dashed, blue, line) which is constant. The approximate behavior $D^\infty \sim \Phi^{3/2}$ represents an over-diffusive transport, unusual for E×B turbulence which is known [6] to exhibit under-diffusive anomalous transport. The presence of RMPs, which in some sense is equivalent with collisions, changes this behavior. The transition from under to over diffusive transport in E × B turbulence in the presence of collisions has been proven before [7]. Fig.6b shows the dependence of the coupling term $D_{\phi b}$ on turbulence amplitude Φ. Two regimes can be delimited: the small and large amplitude turbulence. Since usual turbulence strengths for present day tokamaks, as well for ITER, are ~ 1% one can conclude that the relevant dependency is $D_{\phi b} \sim K_s^2$.

- The effect of RMP amplitude β/B_0 on diffusion coefficients is shown in Fig. 7. The ions are in a regime with $\tau_{eff} \gg \lambda_y/V_p$ thus, the contribution of pure $E \times B$, D_ϕ, is very small. To a good extent one can say that $D \approx D_b + D_{\phi b} \propto D_b^\infty = P_b^2 \Lambda_z^2/P_z$. This analytic dependence (blue, dashed line) is a good fit (Fig. 7) for the numerical results (red circles). A small deviation ≈ 0.05 in the exponent of P_b is revealed. This might be an indicator of a more complicated dependence of $D_{\phi b}$ on β, but the effect is too small to be taken into account. At this end, one can conclude that $D_{\phi b} \propto P_b^2$.

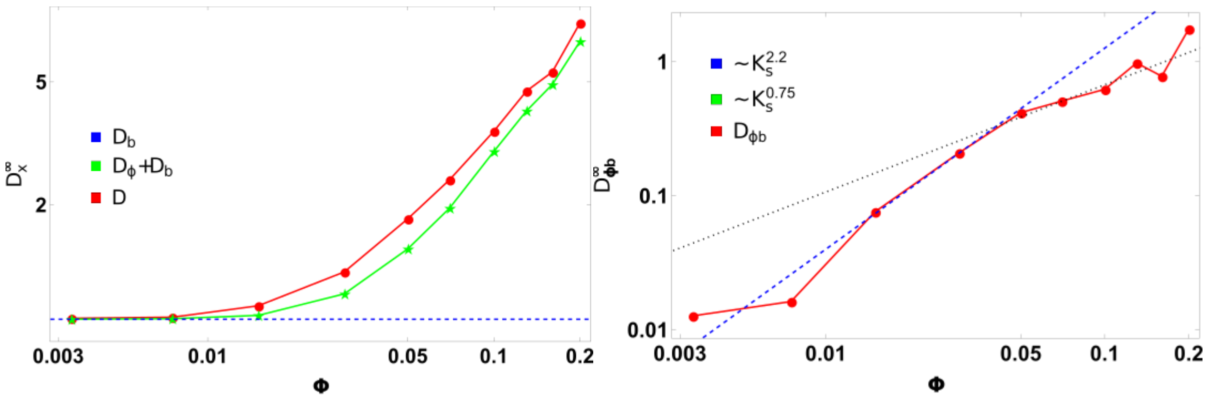

FIG. 2: On Fig. : the left side (a)), asymptotic values of the radial diffusion coefficients versus turbulence amplitude $\Phi = A_\phi e/T_i$. On the right side (b)), the dependence of the coupling term $D_{\phi b}$ on Φ. The simulations are performed in the basic scenario.

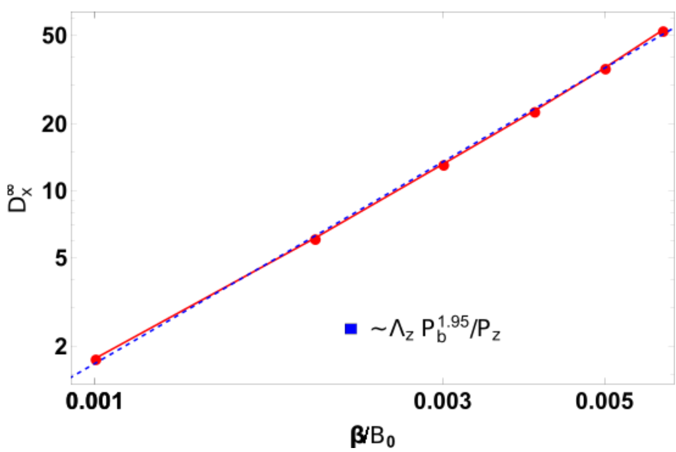

FIG. 3: Asymptotic values of the radial diffusion coefficients versus RMP amplitude β/B_0.

-The effect of poloidal rotations V_p on diffusion coefficients is shown in Fig. 8. The diffusion profile is fitted with a long-range algebraic dependence which decays roughly as V_p^{-2}. The results are in good agreement with previous studies of turbulent transport in different regimes, namely: V_p reduces the radial transport.

- The effect of fast ion thermal energy on transport coefficients is shown in Fig. []. Note that W is directly related to other parameters of the model: the Larmor radius $\rho_f \propto W^{1/2}$, the RMP velocity amplitude $P_b \propto W^{1/2}$ and the effective correlation time $\tau_{eff}^{-2} = \tau_c^{-2} + CW^{1/2}$. Consequently, all components of diffusion, D_ϕ, D_b and $D_{\phi b}$ will be affected by W changes. We can estimate some dependencies using the analysis from Section (IIIA): $D_b^\infty = P_b^2 \Lambda_z P_z^{-1} \propto \sqrt{W}$, $D_\phi \propto f(\rho) \propto \sqrt{W^{-\gamma}}$. Also, at large energies, since $\tau_{eff} \sim W^{-\frac{1}{2}}$ and $D_\phi \sim \tau^{-\gamma_2}$, we expect $D_\phi \propto W^{\frac{\gamma_2-\gamma}{2}}$. Finally, at large values for W energies and τ_c Kubo numbers, we expect:

$$D \approx \left(\frac{\beta L_T}{B_0 \rho_i}\right)^2 W^{\frac{1}{2}} + AW^{0.37} + CW^{0.87}$$

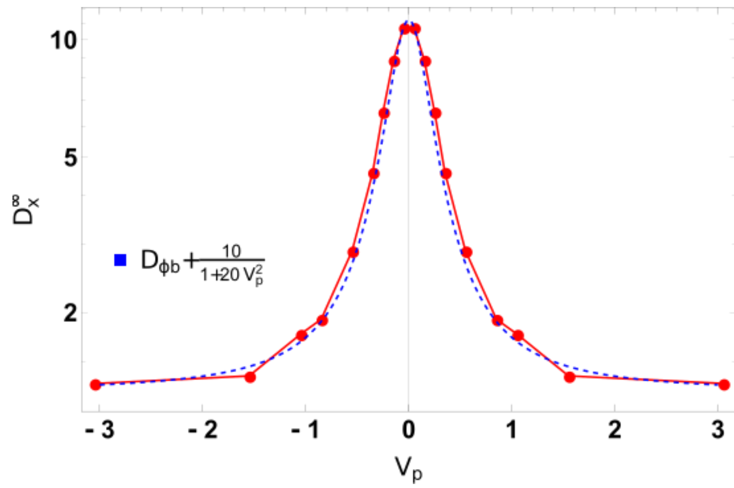

FIG. 4: Asymptotic values of the radial diffusion coefficients versus poloidal velocity V_p. The simulations are performed in the basic scenario.

DNSs were performed in the basic scenario using a correlation time $\tau_c = 5$ and varying the energy W. In Fig. 10a we represent the running diffusion time profiles for several energies. A strong decay of the microscopic transport (at small times) is observed, decay which will affect the asymptotic values. Most likely, this happens because, at small energies, the Larmor radius induced decay of turbulence comes in play faster than the RMP effects which are $\propto W^{1/2}$. In fact, in Fig. 10c, we can see the results of D_ϕ^∞ as a function of energy W (red markers) in the absence of RMP, $\beta = 0$. The decay, which is very similar with the one obtained in the Section (IIIA3) suggests that the effects of τ_{eff} are small. This is supported by the large values of the parallel correlation length of the electrostatic field λ_z. In Fig. 10b the full results regarding the diffusion profile D_x^∞ vs W were represented, alongside with the profile of $D_\phi + D_b^\infty$. Assembling the results from Figs. 10b,10c it can be concluded that, at high energies, the transport is dominated by RMP effects and the turbulence does not matter. Finally, in Fig. 10d is plotted the remainder $D_{\phi b}^\infty$ which exhibits a more complicated dependence on energy, similar with the dependency on turbulence amplitude 6b. Regardless of its shape, the term is at least one order of magnitude smaller than the total diffusion, thus can be neglected across the entire energy spectrum.

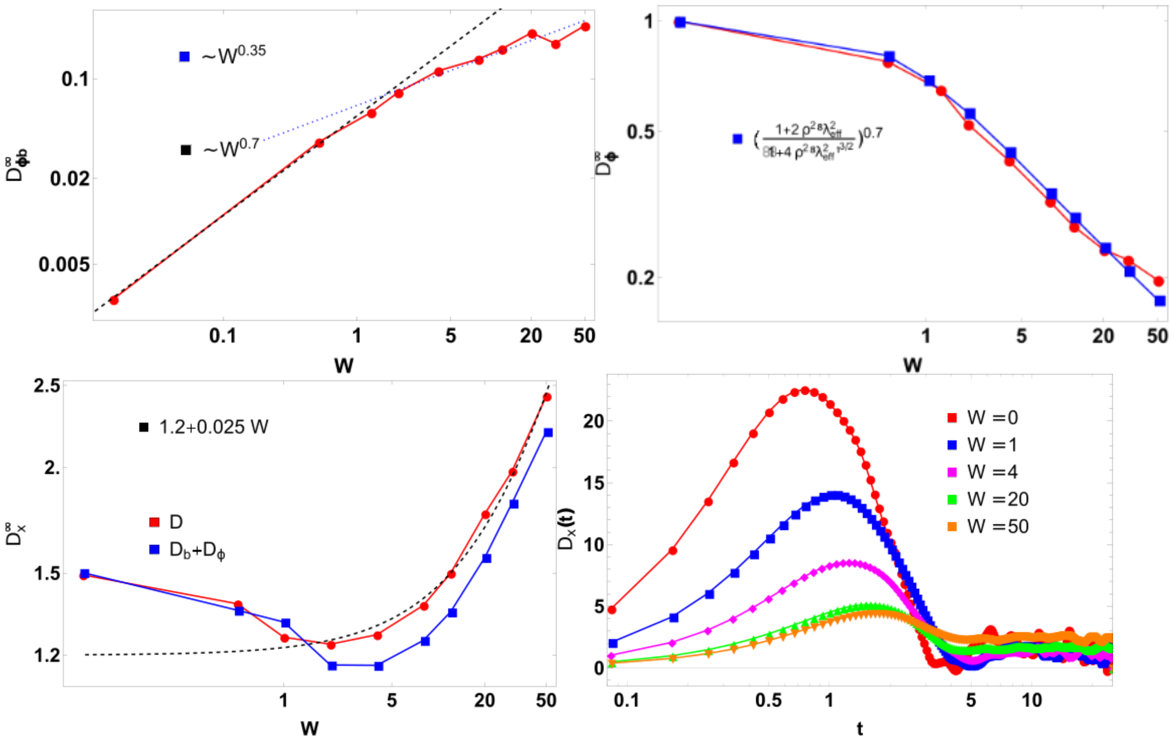

FIG. 5: a) running diffusion time profiles for several energies. b) full asymptotic diffusion dependence on energy. c) Larmor radius effect at work in full non-linear regime. d) energy dependency of the coupling term $D_{\phi b}$.

[1] D.I.Palade, M.Vlad, **arXiv:2006.11106, Statistics and Computing (in press)**

[2] D. I. Palade**, arXiv:2011.02302**

[3] Madalina Vlad, Dragos Iustin Palade, Florin Spineanu**, arXiv:2008.10948**

[4] M. Vlad and F. Spineanu, Nuclear Fusion 56, 092003 (2016)

[5] A. Croitoru, D. Palade, M. Vlad, and F. Spineanu, Nuclear Fusion 57, 036019 (2017)

[6] M. Vlad, F. Spineanu, J. H. Misguich, and R. Balescu, Phys. Rev. E 58, 7359 (1998)

[7] M. Vlad, F. Spineanu, J. H. Misguich, and R. Balescu, Phys. Rev. E 61, 3023 (2000)

Conclusion

T10: Transport and control of W and heavy impurities in the core and SOL.

The main finding of this work is a radial pinch that is generated by the stochastic parallel acceleration in turbulent plasmas. It is significant for high Z impurities and negligible for plasma ions. We have shown that the pinch is produced in three-dimensional turbulence by the interaction of the parallel motion with the HDs, a special type of quasi-coherent radial motion that appears due to a poloidal average velocity. We have also shown that the influence of the parallel motion on the transport through the parallel decorrelation time τ_z^∞ is much stronger for heavy impurities than for plasma ions. The fluctuations of the parallel velocity are very large for W ions, and they determine a smaller parallel decorrelation time that depends on the parameters of the parallel motion $\tau_z^\infty(W, Z, \Phi, \lambda_z)$. This complex decorrelation process influences both the pinch velocity and the diffusion coefficient. It leads to an unusual diffusion regime of super-Bohm type and modifies the scaling laws of V_x^∞ and D_x^∞.

T11: Fast ion confinement, transport and control under ITER relevant conditions.

In this project the effects of resonant magnetic perturbations on the turbulent transport of fast ions in tokamak plasmas were investigated. A minimal transport model of test-particle type has been used to capture the $E \times B$ drift, the parallel motion, the poloidal velocity, inhomogeneous B, finite Larmor radius effects and the RMP fields. The statistical nature of the equations is tackled with a direct numerical simulation method.

The main semi-analytical findings, which are supported by numerical simulations, are:

- inhomogeneous B induces a radial positive pinch $\sim D(t)/R$ which has a fairly small value $\sim 10^{-3} v_{Ti}$
- the Larmor radius effects lead to an algebraic decay of transport $D \sim \rho_f^{-0.75}$
- the pure RMP induces an asymptotic diffusion $P_b^2 \Lambda_z / P_z$
- the non-linear coupling between RMP and $E \times B$ leads to $D \sim \frac{P_b^2 \Lambda_z}{P_z K_s^2} / \lambda_{eff}^2$

$$D_x^\infty = D_\phi^\infty + D_{\phi b}^\infty + D_b^\infty, \qquad D_b^\infty = \frac{P_b^2 \Lambda_z}{P_z}, \quad D_\phi^\infty \propto f(\rho) K_s^\gamma / \tau_{eff}^{\gamma_2[V_p]}$$

,

$$D_{\phi b}^\infty \propto \frac{f(\rho) K_s^2 P_b^2 \Lambda_z W^\gamma}{P_z}, \qquad f(\rho) = \left(\frac{2\rho^2}{\lambda_{eff}^2} + 1\right)^\gamma \left(\frac{4\rho^2}{\lambda_{eff}^2} + 1\right)^{-\frac{3\gamma}{2}}$$

Papers

[*] D. I. Palade, M. Vlad, *Fast generation of Gaussian random fields for direct numerical simulations of stochastic transport*, *Statistics and computing* (in press)

[**] M. Vlad, D. I. Palade, F. Spineanu, Effects of the parallel acceleration on heavy impurity transport in turbulent tokamak plasmas, *2020, arxiv: 2008.10948, submitted to Plasma Phys. Control. Fusion*

[***] D. I. Palade, *Turbulent transport of fast ions in tokamak plasmas in the presence of resonant magnetic perturbations,* arXiv:2011.02302, submitted to Physics of Plasmas

Conferences

[1] D. I. Palade, M. Vlad, F. Spineanu, *Turbulent Transport of the W Ions in Tokamak Plasmas,* IAEA Fusion Energy Conference (FEC) 2020, Nice, May 2021

[2] D. I. Palade, M. Vlad, F. Spineanu, Turbulent transport control by tokamak plasma rotation, Chaotic Modelling and Simulation International Conference CHAOS 2020 (virtual).

MST1 Task Force Meeting presentations

1. D. I. Palade, 06/04/2020, *Discrete representations of Gaussian Random Fields for Direct Numerical Simulations of stochastic transport*
2. M. Vlad, D. I. Palade, F. Spineanu, 28/06/2020, *Effects of the parallel acceleration on heavy impurity transport in turbulent tokamak plasmas*